PLANNING MALAYSIA:
Journal of the Malaysian Institute of Planners
VOLUME 21 ISSUE 6 (2023), Page 57 – 71

CHANGING EXTREME SEA LEVELS ALONG THE COAST OF MALAYSIA

Abd Muhaimin Amiruddin[1], Iszuanie Syafidza Che Ilias[2], Muhamad Kasturi Mohd Dallye[3], Latifah Abd Manaf[4], Khairul Nizam Mohamed[5]

[1,4,5]*Faculty of Forestry and Environment,*
[2,3]*Institute for Mathematical Research,*
UNIVERSITI PUTRA MALAYSIA

Abstract

This study examined extreme sea level (ESL) variations along the Malaysian coast using hourly sea level data from 17 tide gauge stations. The maximum observed ESLs varied from 1.26 m at Bintulu to 2.92 m at Port Klang, with tides playing a significant role in ESLs, especially along the west coast of Peninsular Malaysia. The spatial variation of seasonal ESLs showed a higher maximum of non-tidal residuals (0.8-1.1 m) along the east coast of Peninsular Malaysia during the northeast monsoon. This can be mainly attributed to the influence of the monsoon wind. Moreover, significant increases in ESLs were observed at 14 stations, largely due to rises in mean sea level. The interannual variability of ESL could be associated with the El Niño-Southern Oscillation at most sites except the northeast coast of Peninsular Malaysia. Interestingly, the interannual variability of the non-tidal residuals could be linked to the monsoon at sites located on the west coast of Peninsular Malaysia and East Malaysia. These findings provide valuable insights to relevant authorities for coastal planning, especially regarding flood risk management and the formulation of effective mitigation strategies.

Keywords: South China Sea, Malacca Strait, Extreme Sea-Level, Sea-Level Rise, Tides.

[1] Corresponding author. Email: muhai@upm.edu.my

INTRODUCTION

Extreme sea level (ESL) is the occurrence of an unusually high or low local sea surface driven by short-term events, including tides, storm surges, waves, and seiches (Gregory et al. 2019). Based on the tide gauge observations, the changes in extreme still water level (combination between relative mean sea level, tide, and surge) at most locations globally are primarily driven by relative mean sea level (MSL) rise (Oppenheimer et al., 2019). ESL is affected by relative sea-level changes in two ways: directly by moving average water levels and indirectly by modifying the depth at which tides, waves, and surges propagate (Pickering et al., 2012).

The planning of coastal protection at local and regional levels requires a detailed understanding of the spatial and temporal characteristics of ESL and their possible mechanisms (Wahl et al., 2017). In evaluating overall risk, coastal planners need to know the likelihood of flooding in addition to the value of assets and communities that may be affected. For instance, by analyzing extreme sea level distributions, planners can determine how often specific levels may be surpassed in any given year, representing the Return Period (or Average Recurrence Interval) for a particular level at a specific location (Woodworth 2022). As global sea level is expected to continuously rise beyond the end of this century (Fox-Kemper et al., 2021), this will lead to an increase of frequency and severity of ESL and coastal flooding, particularly in tropical regions (Oppenheimer et al., 2019).

Located in tropical Southeast Asia, Malaysia is surrounded by the South China Sea (SCS), the Sulu Sea, the Celebes Sea, and the Malacca Strait. In 2020, about 5.9 million people (excluding Sabah and Sarawak) mostly lived in 16 major cities located in the Malaysian coastal zone (PLANMalaysia, 2022). Economically, about 40 per cent of Malaysia's gross domestic product (GDP) is attributed to the maritime industry (MIDA, 2021). In particular, Port Klang and Port of Tanjung Pelepas, located on the west and south coasts of Peninsular Malaysia respectively, were included in the top 15 global container ports for the year 2019-2020 (UNCTAD, 2021). Therefore, the increase in ESL and the associated coastal flooding will severely threaten the high coastal population and economic importance of this region.

In investigating the ESL characteristics over the whole SCS, Pham et al. (2019) showed that the maximum ESLs vary spatially between 0.9 m and 4 m. They suggested that the spatial variability of ESLs in southern China is largely due to the summer tropical cyclones, which is in agreement with the findings by Feng and Tsimplis (2014) and Zhang and Sheng (2015). In the southern SCS, Pham et al. (2019) suggested that ESLs are primarily driven by different forcings associated with the winter monsoonal wind. They also found a significant link between ESL in the SCS and the two climate modes of the Pacific Decadal

Oscillation and the El Niño-Southern Oscillation (ENSO). Nevertheless, to date, understanding the long-term characteristics and seasonal variations of ESL, especially along the Malaysian coast, is still far from complete. The temporal variability of ESLs and their link to the climate modes of ENSO, the Indian Ocean Dipole (IOD), and the monsoon are still unresolved.

The general aim of this study was to assess the changes in ESLs along the Malaysian coast using tide gauge records and explore their link to climate modes. The first specific objective was to evaluate the spatial distributions of the maximum ESL, their seasonal variations, and sea level return periods. Then, the temporal variability of ESL was examined, including its link to regional climate indices.

RESEARCH METHODOLOGY

Data

Hourly sea level data from 17 tide gauges were primarily obtained from the University of Hawaii Sea Level Center (UHSLC) (Caldwell et al., 2015) except for one site at Labuan (sites 16), which was obtained from Department of Survey and Mapping Malaysia (Figure 1). The sea level data consist of more than 22 years long and spanning over different periods between 1983 and 2019. Quality control was carried out by visually inspecting each time series. The time series was carefully processed to eliminate any erroneous data points caused by phase offset, datum shift, or data spikes. Additionally, the tide gauge records at Pulau Langkawi, Pulau Pinang, and Lumut stations in the northern Malacca Strait showed non-climatic signals resulting from the 2004 Sumatra-Andaman earthquake-driven tsunami, which were also appropriately removed from the analysis.

Three climate indices, namely the Oceanic Niño Index (ONI), the Dipole Mode Index (DMI), and the Western North Pacific Monsoon Index (WNPMI), were used to examine the influence of climate modes on the temporal variability of ESL at interannual scale. The ONI was represented by the 3-month average temperature anomaly in the surface waters of the east-central tropical Pacific (Barnston et al., 1997). The differences in sea surface temperature anomalies between the western and eastern regions of the equatorial Indian Ocean formed the basis of the DMI (Saji et al., 1999). The WNPMI was inferred from the differences in the 850-hPA zonal wind between a southern region (5º-15ºN, 100º-130ºE) and a northern region (20º-30ºN, 110-140E) (Wang & Fan, 1999).

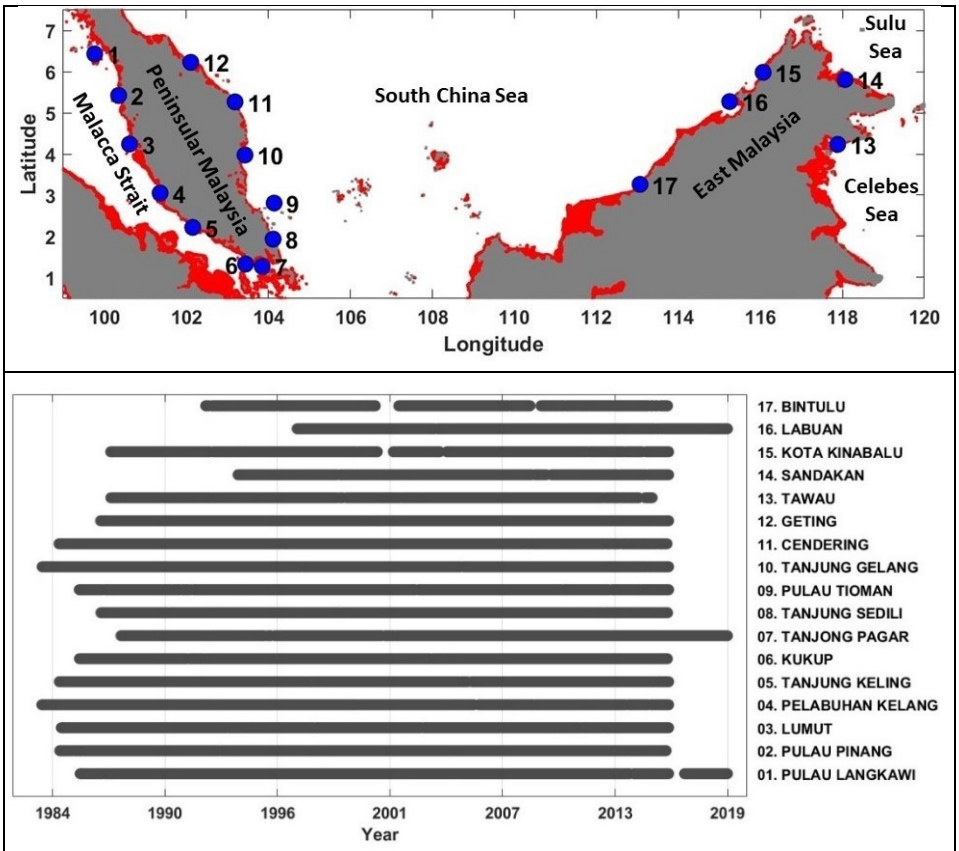

Figure 1. The location of selected tide gauge stations (top) and the available data period for each station (bottom). The red colour indicates the low-lying areas between 0 and 5 m above mean sea level

METHODOLOGY

To account for potential variations in station datum (benchmark or reference level) between different countries, the observed records at each site were adjusted by referencing them to their respective average sea level records across the entire available period. Subsequently, the observed sea level records were further decomposed into three primary components: mean sea level (MSL), tidal variations, and the non-tidal residual (NTR).

Based on the harmonic analysis, the tidal components were computed using the T_TIDE software package (Pawlowicz et al., 2002). For each calendar year with a minimum of 75% of valid data, the tidal signal has been calculated taking into account 65 tidal constituents. As the annual and semi-annual are

mainly driven by meteorological factors, these components were omitted from the computation of tides.

After calculating the tidal components, they were subtracted from the observed sea level at each tide gauge station, resulting in the derivation of the NTR. Additionally, the mean spring tidal range was computed based on the average differences between the monthly maximum and minimum levels of spring tides. To assess the spatial distribution of seasonal variations in ESL, the observed ESL and the NTR were divided into two seasons: the Northeast Monsoon (Oct-Mac) and the Southwest Monsoon (Apr-Sep).

The direct peak over threshold (POT) method was employed to estimate the probabilities of ESL. Compared to other direct methods such as r-largest events and block maxima, the POT method is considered more effective as the chosen extreme values are based on a reasonable upper threshold rather than being constrained by a fixed number of extreme values per year (Arns et al., 2013). Hence, the risk of losing actual extreme events in the chosen criteria can be reduced.

In addition, the probability of extreme sea level (ESL) events was also estimated using the Generalized Pareto Distribution (GPD). Following Coles (2001), the extreme values that surpassed a specified threshold based on the POT method were then fitted to the GPD, which followed the cumulative distribution function:

$$GPD(y) = 1 - (1 + \frac{\xi y}{\theta})^{-1/\xi} \text{ , with } \theta = \sigma + \xi(u - \mu) \quad \text{Eq. 1}$$

Where σ is a scale parameter, ξ is a shape parameter, μ is a location parameter, u is the threshold, and y is the number of independent extreme values that exceed the threshold. As recommended by Coles (2001), the maximum likelihood approach was employed to estimate the shape and scale parameters.

To eliminate the influence of long-term mean sea level (MSL) changes on extreme event probabilities, a linear trend was calculated based on the annual MSL data and then subtracted from the observed sea level records at each station. This was done before calculating the daily maxima.

The selection of an appropriate threshold is crucial to accurately assessing the tail distribution of sea level and capturing an adequate number of real extreme events. To investigate the sensitivity of threshold selection, various percentiles were considered, including the 99th, 99.3rd, 99.5th, and 99.7th percentiles.

After analysing the stability of the Generalized Pareto Distribution (GPD) parameters, notably the shape parameter (ξ), the threshold was set at the 99.3th percentile of the available sea level records at each station. To ensure independence between extreme events, a time period of 96 hours was chosen between successive events.

The return period refers to an estimation of the average time, in years, between occurrences of extreme events of a specific level being exceeded at a particular location. The N-year return level (R) of an extreme event was defined as:

$$R = u + \frac{\sigma}{\xi}(N^{\xi} - 1) \quad \text{Eq. 2}$$

Based on the delta method recommended by Coles (2001), the uncertainty related to the estimated return levels was determined at a 95% confidence interval.

To investigate the inter-annual and long-term variability and trends in ESL, a percentiles analysis was employed. Annual percentiles were calculated using both the observed sea level and the NTR data available during the study period. This involved sorting the sea level and NTR data in increasing order and finding the values corresponding to specific percentiles. The 99th and 99.9th percentiles were chosen to assess changes in ESL. Additionally, the 50th percentile, representing the annual MSL, was computed to provide insights into the average sea level behaviour over the study period. Trends in percentiles were calculated using linear regression. The inter-annual variability of ESL percentiles was correlated with three climate indices (ONI, DMI, and WNPMI). The statistical significance of the linear trends and the correlation analysis were assessed at the 95% confidence interval.

ANALYSIS AND DISCUSSION

The Spatial Distribution of Extreme Sea Level

Over the whole available record, the maximum observed ESL at each site, varied between 1.26 m at Bintulu (Site 17) and 2.92 m at Pelabuhan Kelang (Site 4) (Figure 1a). The largest range of maximum ESL values was observed on the west coast of Peninsular Malaysia and was between 1.56 m and 2.92 m, whereas the smaller range was located in the southeastern SCS between 1.26 m and 1.5 m. The maximum observed ESL values consisted of the combined contributions from MSL, tidal variations, and the NTR components. Together, these factors determined the highest sea level experienced at a given location during extreme events.

To examine the role of tides in ESLs, the mean spring tidal range was estimated at each site. The mean spring tidal range showed high spatial variation (Figure 1b), varying between 1.12 m at Geting (Site 12) and 5 m at Pelabuhan Kelang (Site 4). The mean spring tidal range at Pelabuhan Kelang was notably larger when compared to the neighbouring sites on the west coast of Peninsular Malaysia (2.22-3.38 m). This could be associated with the narrowing shapes from

the northern Malacca Strait to the middle part of the Malacca Strait and Pelabuhan Kelang, which can create a funnelling effect and thus amplify the tidal range.

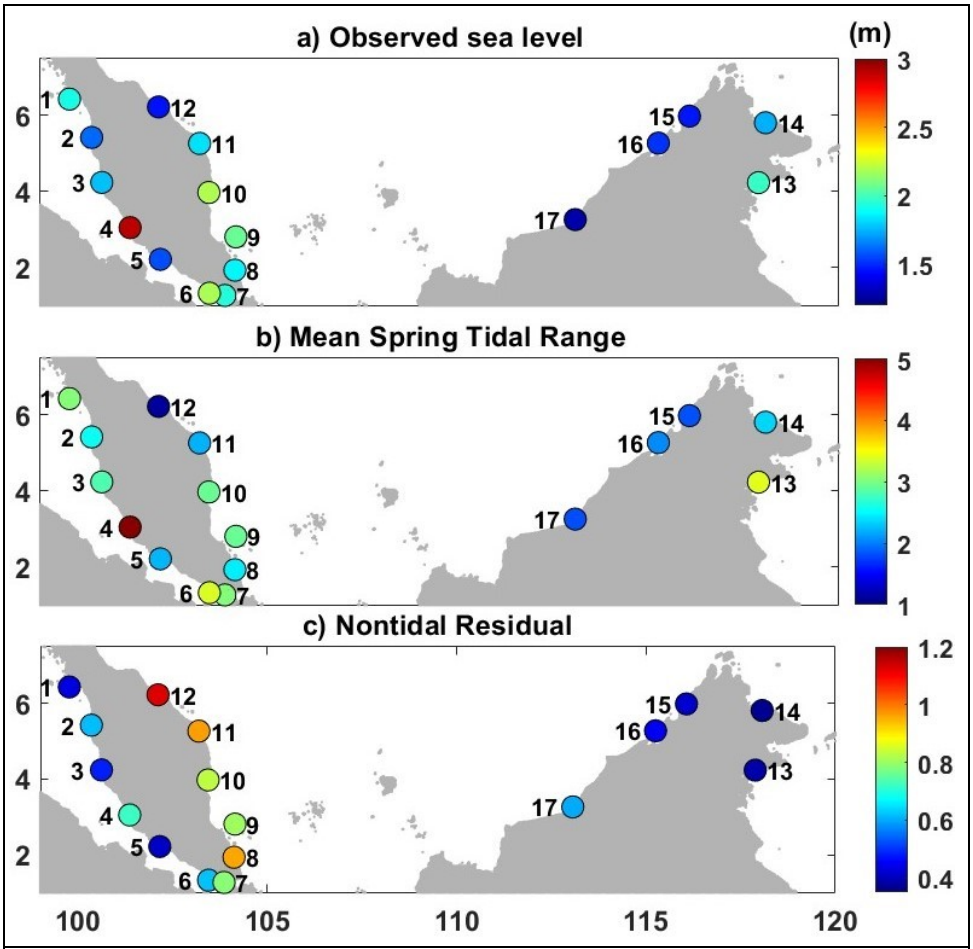

Figure 2. Spatial distribution of maximum observed sea level(a), mean spring tidal range (b) and maximum nontidal residual (c).

The NTR component was estimated by subtracting the tidal component from the observed ESL. The maximum NTR varied between 0.37 m at Sandakan (Site 14) and 1.13 m at Geting (Site 12). On the west coast of Peninsular Malaysia, it is interesting to observe that ESL values exhibited considerable variation, with differences reaching up to 1.4 meters. However, in contrast, the maximum NTR values demonstrated close agreement, ranging from 0.4 to 0.7 meters. This finding suggests a substantial contribution of tides to the overall extreme sea level in this region.

The maximum ESLs and NTRs were divided into two seasons, namely: the Northeast Monsoon (Oct-Mac) and the Southwest Monsoon (Apr-Sep), to assess the seasonal variations in ESLs. Most sites showed that the maximum seasonal ESLs were observed during the Northeast Monsoon (Figure 3). In particular, the differences between these two monsoons for the maximum observed ESL (Figure 3a) and NTR (Figure 3b) were higher, ranging between 0.36 m and 0.8 m on the west coast of Peninsular Malaysia. This could be linked to the forcing of monsoon winds in the southwestern SCS (Amiruddin et al., 2015). The smaller differences between these two monsoons for the maximum observed ESL and NTR were observed on the west coast of Peninsular Malaysia, which were less than 0.16 m.

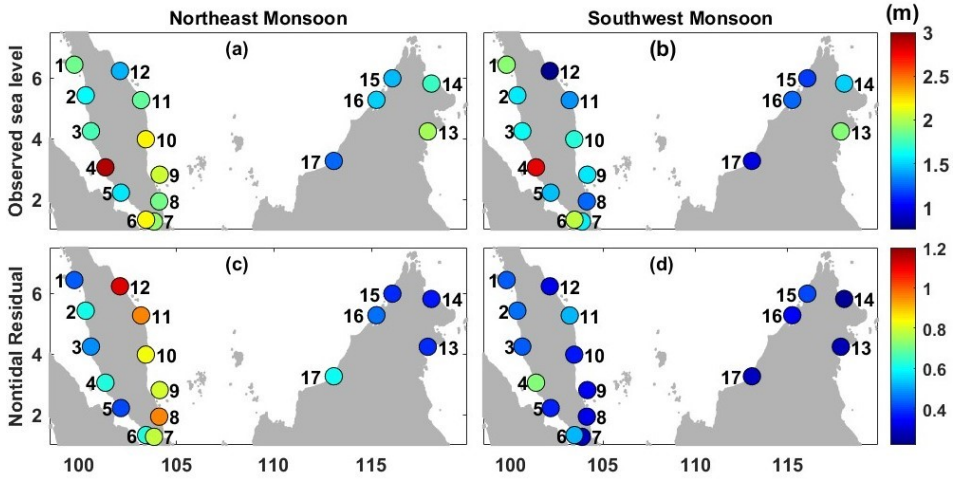

Figure 3. Spatial distribution of maximum observed sea level (top) and nontidal residual (bottom) during northeast monsoon (left) and southwest monsoon (right).

Return periods indicate the average time between a particular sea level return level being exceeded at a specific location, enabling coastal planners, engineers, and policymakers to assess the probability and severity of extreme events like flooding (Wahl et al., 2017). Using the 99.3th percentile threshold, the 50- and 100-year return levels for ESLs and the NTR were estimated and listed in Table 1. The 50-year ESL return levels varied between 1.3 m at Bintulu (Site 17) and 2.92 m at Pelabuhan Kelang (Site 4). The 100-year ESL return levels ranged between 1.38 m and 2.95 m at the same sites. For the NTR, the 50-year return levels varied between 0.36 m at Sandakan (Site 14) and 1.16 m at Geting (Site 25). The 100-year NTR return levels ranged between 0.37 m and 1.29 m at the same sites. Note that the large uncertainty (>1 m) at Bintulu for the

NTR return level might be related to the deficiency of the assumed probability distribution and lead to low confidence in the model projection.

Table 1. The 50-year and 100-year return levels for the observed ESL and the NTR.

	Station Name	Observed ESL		NTR	
		50 year (m)	100 year (m)	50 year (m)	100 year (m)
1	Pulau Langkawi	1.91 (0.09)	1.94 (0.12)	0.43 (0.03)	0.44 (0.03)
2	Pulau Pinang	1.56 (0.08)	1.60 (0.11)	0.56 (0.09)	0.59 (0.12)
3	Lumut	1.74 (0.09)	1.77 (0.11)	0.45 (0.05)	0.47 (0.07)
4	Pelabuhan Kelang	2.92 (0.10)	2.95 (0.13)	0.72 (0.16)	0.77 (0.22)
5	Tanjung Keling	1.56 (0.09)	1.59 (0.11)	0.42 (0.03)	0.43 (0.04)
6	Kukup	2.15 (0.06)	2.17 (0.07)	0.58 (0.07)	0.61 (0.09)
7	Tanjong Pagar	1.93 (0.31)	2.07 (0.50)	0.76 (0.15)	0.81 (0.20)
8	Tanjung Sedili	1.87 (0.30)	1.98 (0.44)	1.04 (0.30)	1.15 (0.43)
9	Pulau Tioman	2.04 (0.15)	2.09 (0.20)	0.78 (0.11)	0.82 (0.15)
10	Tanjung Gelang	2.12 (0.12)	2.17 (0.15)	0.84 (0.16)	0.90 (0.22)
11	Cendering	1.85 (0.17)	1.91 (0.23)	0.90 (0.16)	0.96 (0.21)
12	Geting	1.48 (0.26)	1.59 (0.39)	1.16 (0.33)	1.29 (0.49)
13	Tawau	1.97 (0.04)	1.98 (0.04)	0.42 (0.13)	0.47 (0.20)
14	Sandakan	1.71 (0.19)	1.78 (0.28)	0.36 (0.03)	0.37 (0.03)
15	Kota Kinabalu	1.44 (0.22)	1.52 (0.33)	0.41 (0.03)	0.42 (0.04)
16	Labuan	1.62 (0.43)	1.76 (0.69)	0.44 (0.04)	0.45 (0.05)
17	Bintulu	1.30 (0.24)	1.38 (0.34)	0.82 (0.72)	1.04 (1.25)

*The standard error (95% confidence interval are stated in bracket

Temporal Variability of Extreme Sea Level

To determine the temporal changes of ESLs and the link with climate modes, the 50th, 99th, and 99.9th percentiles were estimated for all sites. Using linear regression, trends in each of the 50th, 99th, and 99.9th percentiles, were computed and listed in Table 2. Positive significant trends in the 99th and 99.9th ESL percentiles were found at 10 and 9 sites, respectively. The largest trend in the 99th percentile was 4.5 ± 1.7 mm/yr at Pelabuhan Kelang (Site 4). For the 99.9^{th} percentile, the largest trend was 5.8 ± 5.4 mm/yr at Sandakan (Site 17). It is important to understand that the substantial differences in trends observed for each site could be attributed, in part, to the variation in the periods of the available records at each location. The varying available records for each site contributed to the diverse trends observed, making it essential to consider the record length when interpreting and comparing the results from different tide gauge stations.

The available records for the stations on the west coast and the east coast of Peninsular Malaysia spanned over the common period of 1983-2015, allowing direct comparison of trends among sites. On the west coast of Peninsular Malaysia, the trends of the 99th percentile were significant at all sites. The

significant positive trends varied between 1.7 ± 1.6 mm/yr at T. Keling (Site 5) and 4.5 ± 1.7 mm/yr at P. Kelang (Site 4). On the east coast of Peninsular Malaysia, a significant trend in the 99th percentile was only observed at Geting (Site 12) and T. Pagar (Site 7), both about 3.4 mm/yr. Insignificant trends were observed at most sites (not shown) after subtracting the 50th percentile from the 99th and 99.9th percentiles. This suggests that trends observed in ESLs at most stations were due to the rise observed in MSL, in agreement with studies in the South China Sea from Feng and Tsimplis (2014) and Pham et al. (2019).

Table 2. Linear trends of sea level percentiles over available records

	Station Name	Observed sea level trends (mm/yr)		
		50th	99th	99.9th
1	Pulau Langkawi	**3.5 ± 1.5**	**3.0 ± 1.3**	**3.0 ± 1.9**
2	Pulau Pinang	**3.3 ± 1.5**	**2.4 ± 1.3**	1.5 ± 2.1
3	Lumut	**2.8 ± 1.4**	**2.4 ± 1.3**	2.0 ± 2.2
4	Pelabuhan Kelang	**2.6 ± 1.5**	**4.5 ± 1.7**	**5.0 ± 4.1**
5	Tanjung Keling	**1.9 ± 1.6**	**1.7 ± 1.6**	2.1 ± 2.3
6	Kukup	**3.0 ± 1.7**	**4.1 ± 1.3**	**5.8 ± 1.8**
7	Tanjong Pagar	**3.3 ± 1.7**	**3.4 ± 1.7**	**3.1 ± 2.4**
8	Tanjung Sedili	0.9 ± 2.0	0.0 ± 2.4	2.2 ± 3.8
9	Pulau Tioman	**2.2 ± 1.4**	1.2 ± 2.5	2.9 ± 3.4
10	Tanjung Gelang	1.6 ± 1.9	1.2 ± 2.6	**3.7 ± 2.9**
11	Cendering	1.6 ± 1.8	1.3 ± 2.7	1.5 ± 3.8
12	Geting	**2.2 ± 1.7**	**3.4 ± 2.0**	**4.7 ± 4.0**
13	Tawau	**4.3 ± 2.2**	**3.8 ± 1.9**	**4.1 ± 2.2**
14	Sandakan	**2.5 ± 2.4**	**3.3 ± 4.6**	**5.8 ± 5.4**
15	Kota Kinabalu	**3.7 ± 1.5**	2.7 ± 2.8	**4.4 ± 4.0**
16	Labuan	**3.1 ± 2.2**	2.3 ± 4.3	2.7 ± 6.2
17	Bintulu	**2.5 ± 1.8**	3.1 ± 4.0	3.9 ± 5.4

*The statistically significant trends are shown in bold

To examine the connection between inter-annual variability in ESLs and climate modes, the 99th ESL percentile time-series at each site were correlated with three climate indices, namely: the ONI, the DMI, and the WNPMI. The 99th percentiles of observed ESL were significantly anti-correlated with the ONI at most sites, except at three sites (Tg. Gelang, Cendering and Geting), all located on the northeast coast of Peninsular Malaysia (Table 3). The 99th percentiles of the observed ESL were also significantly anti-correlated with the DMI, but only at the four sites (Pulau Langkawi, Pulau Pinang, Lumut, and Kelang) located on the northwest coast of Peninsular Malaysia. For the WNPMI, the distinct significant correlations were found with the 99th ESL NTR percentiles at five sites on the west coast of Peninsular Malaysia (except Pulau Langkawi) and five sites located in East Malaysia. The results indicate the link between La Nina, the

negative modes of Indian Ocean Dipole and Monsoon in modulating the positive ESL in certain areas of the region.

Table 3. Correlation coefficient between 99th percentiles of observed extremes with ONI and DMI, and 99th percentile of NTR with WNPMI

	Station Name	ONI	DMI	WNPMI
1	Pulau Langkawi	-0.35	-0.40	
2	Pulau Pinang	-0.59	-0.47	-0.41
3	Lumut	-0.73	-0.49	-0.47
4	Pelabuhan Kelang	-0.55	-0.35	-0.45
5	Tanjung Keling	-0.56		-0.74
6	Kukup	-0.50		-0.71
7	Tanjong Pagar	-0.63		
8	Tanjung Sedili	-0.42		
9	Pulau Tioman	-0.43		
13	Tawau	-0.73		-0.43
14	Sandakan	-0.49		-0.86
15	Kota Kinabalu	-0.37		-0.71
16	Labuan	-0.67		-0.81
17	Bintulu	-0.67		-0.46

*Only statistically significant correlations are shown

SUMMARY AND CONCLUSION

The changes of ESLs and the NTR were examined using 17 tide gauge stations along the Malaysia coast. Maximum ESLs varied between 11.26 m at Bintulu and 2.92 m at Pelabuhan Kelang. The maximum NTR varied between 0.37 m at Sandakan and 1.13 m at Geting, indicating substantial influence of tides to the ESL, especially on the west coast of Peninsular Malaysia. Changes of tides have been observed worldwide (Talke and Jay, 2020; Haigh et al., 2020). The rise and fall of tides reaching higher levels due to elevated MSL will result in an escalated risk of coastal flooding. Changes in the characteristics of tides in Malaysia needs to be explored in the future studies.

The maximum values of ESLs were observed along Malaysia coast, primarily during the Northeast Monsoon. During this period, the risk of coastal flooding is notably larger for potentially vulnerable sites, especially when considering the combination of factors such as the maximum mean seasonal sea level cycle, high spring tide, storm surge, and heavy rainfall. Understanding the interplay of these factors is crucial for effective coastal management and preparedness to mitigate the impacts of extreme events and compound flooding in coastal regions.

The positive significant trends in ESL percentiles were observed to be primarily attributed to variations in MSL. The inter-annual ESL variability was found to be linked to ENSO at most sites except the northeast coast of Peninsular

Malaysia. Interestingly, this study found that the inter-annual variability of the NTR on the west coast of Peninsular Malaysia, and sites in East Malaysia can be connected with the monsoon. Understanding mechanisms of the climate modes in influencing the changes of extremes in these regions should be explored in the future studies.

In conclusion, this study has provided an output of spatial and temporal variation of ESL along the coast of Malaysia. As the frequency of coastal flooding is expected to rise exponentially due to mean sea level rise (Taherkhani et al., 2020), this information is highly beneficial in recognising vulnerable coastal areas that face an increased probability of experiencing ESLs. In particular, the estimated return periods computed at each site offer valuable parameters for coastal planning and the design of flood defence measures along the coast. Moreover, the study's findings, especially concerning temporal variability, provide crucial insights for modelling future changes in ESLs along the Malaysian coast. This information proves indispensable for relevant authorities in implementing effective mitigation strategies, as well as disaster risk reduction and management measures (e.g. Amin & Hashim, 2014; Chong & Kamarudin, 2018) against coastal flooding, including sustainable coastal planning and development.

ACKNOWLEDGEMENT

This project was supported by Universiti Putra Malaysia under the Putra Young Initiative (IPM) Grant (GP-IPM/2018/9654300) and Institute for Mathematical Research (INSPEM), Universiti Putra Malaysia through Agricultural and Environment with Computational Intelligence Funding Initiative (INSPEM/AECIFI/1/2021/6233205).

DATA AVAILABILITY

Hourly tide gauge records are available from University of Hawaii Sea Level Center (UHSLC) (http://www.uhslc.soest.hawaii.edu). Climate indices of ONI is available from National Oceanic and Atmospheric Administration (NOAA) (https://www.cpc.ncep.noaa.gov/data/indices/oni.ascii.txt), DMI is available from Japan Agency for Marine-Earth Science and Technology JAMSTEC (https://www.jamstec.go.jp/aplinfo/sintexf/iod/dipole_mode_index.html) and WNPMI is available from Asia Pacific Data Research Center (APDRC) (http://apdrc.soest.hawaii.edu/projects/monsoon/seasonal-monidx.html).

REFERENCES

Amin, I. A. M., & Hashim, H. S. (2014). Disaster risk reduction in Malaysia urban planning. *Planning Malaysia*, 12, 35–38. https://doi.org/10.21837/pm.v12i4.124

Amiruddin, A. M., Haigh, I. D., Tsimplis, M. N., Calafat, F. M., & Dangendorf, S. (2015).

The seasonal cycle and variability of sea level in the South China Sea. *Journal of Geophysical Research: Oceans*, *120*(8), 5490–5513. https://doi.org/https://doi.org/10.1002/2015JC010923

Arns, A., Wahl, T., Haigh, I. D., Jensen, J., & Pattiaratchi, C. (2013). Estimating extreme water level probabilities: A comparison of the direct methods and recommendations for best practise. *Coastal Engineering*, *81*, 51–66. https://doi.org/10.1016/j.coastaleng.2013.07.003

Bamston, A. G., Chelliah, M., & Goldenberg, S. B. (1997). Documentation of a highly ENSO-related sst region in the equatorial pacific: Research note. *Atmosphere-Ocean*, *35*(3), 367–383. https://doi.org/10.1080/07055900.1997.9649597

Caldwell, P. C., Merrifield, M. A., & Thompson, P. R. (2015). Sea level measured by tide gauges from global oceans—The Joint Archive for Sea Level holdings (NCEI Accession 0019568), Version 5.5. *NOAA National Centers for Environmental Information*, Dataset, doi:10.7289/V5V40S7W

Chong, N. O., & Kamarudin, K. H. (2018). Disaster risk management in Malaysia: Issues and challenges from the perspective of agencies. *Planning Malaysia*, *16*(1), 105–117. https://doi.org/10.21837/pmjournal.v16.i5.415

Coles, S., (2001). *An Introduction to Statistical Modelling of Extreme Values*. Springer. (207pp.).

Feng, X., & Tsimplis, M. N. (2014), Sea level extremes at the coasts of China, *Journal of Geophysical Research: Oceans*, *119*(3), 1593-1608, doi: http://dx.doi.org/10.1002/2013JC009607.

Fox-Kemper, B., Hewitt, H. T., Xiao, C., Aðalgeirsdóttir, G., Drijfhout, S. S., Edwards, T. L., et al. (2021). Ocean, Cryosphere and Sea Level Change. *Climate Change 2021: The Physical Science Basis. Contribution of Working Group I to the Sixth Assessment Report of the Intergovernmental Panel on Climate Change*, Cambridge University Press.

Gregory, J. M., Griffies, S. M., Hughes, C. W., Lowe, J. A., Church, J. A., Fukimori, I., … van de Wal, R. S. W. (2019). Concepts and Terminology for Sea Level: Mean, Variability and Change, Both Local and Global. In *Surveys in Geophysics* (Vol. 40). https://doi.org/10.1007/s10712-019-09525-z

Haigh, I. D., Pickering, M. D., Green, J. A. M., Arbic, B. K., Arns, A., Dangendorf, S., … Woodworth, P. L. (2020). The Tides They Are A-Changin': A Comprehensive Review of Past and Future Nonastronomical Changes in Tides, Their Driving Mechanisms, and Future Implications. *Reviews of Geophysics*, *58*(1), 1–39. https://doi.org/10.1029/2018RG000636

MIDA [Malaysian Investment Development Authority] (2021). Revitalising the Maritime Industry Through Blue Economy. *MIDA e-Newsletter February 2021.* Retrieved from https://www.mida.gov.my/e-newsletters/e-newsletters-years/2021/

Oppenheimer, M., B.C. Glavovic , J. Hinkel, R. van de Wal, A.K. Magnan, A. Abd-Elgawad, R. Cai, M. Cifuentes-Jara, R.M. DeConto, T. Ghosh, J. Hay, F. Isla, B. Marzeion, B. Meyssignac, and Z. Sebesvari, (2019): Sea Level Rise and Implications for Low-Lying Islands, Coasts and Communities. *In: IPCC Special Report on the Ocean and Cryosphere in a Changing Climate* [H.-O. Pörtner, D.C. Roberts, V. Masson-Delmotte, P. Zhai, M. Tignor, E. Poloczanska, K.

Mintenbeck, A. Alegría, M. Nicolai, A. Okem, J. Petzold, B. Rama, N.M. Weyer (eds.)]

Pawlowicz, R., Pawlowicz, R., Beardsley, R. C., Beardsley, R., Lentz, S., & Lentz, S. (2002). Classical tidal harmonic analysis including error estimates in MATLAB using T-TIDE. *Computers & Geosciences*, *28*(8), 929–937. Retrieved from http://www.ocgy.ubc.ca/~rich.

Pham, D. T., Switzer, A. D., Huerta, G., Meltzner, A. J., Nguyen, H. M., & Hill, E. M. (2019). Spatiotemporal variations of extreme sea levels around the South China Sea: assessing the influence of tropical cyclones, monsoons and major climate modes. *Natural Hazards, 98,* 969-1001. https://doi.org/10.1007/s11069-019-03596-2

PLANMalaysia, (2022). *Rancangan Fizikal Zon Pesisiran Pantai Negara-2, Jilid 1 Strategi Pengurusan Persisiran Pantai Negara*. Federal Department of Town and Country Planning (PLANMalaysia), Kuala Lumpur. https://www.planmalaysia.gov.my/index.php/en/rancangan-fizikal-zon-pesisiran-pantai-negara-2

Pickering, M. D., Wells, N. C., Horsburgh, K. J., & Green, J. A. M. (2012). The impact of future sea-level rise on the European Shelf tides. *Continental Shelf Research*, *35*, 1–15. https://doi.org/10.1016/j.csr.2011.11.011

Saji, N. H., Goswami, B. N., Vinayachandran, P. N., & Yamagata, T. (1999). A dipole mode in the tropical Indian Ocean. *Nature*, *401*(6751), 360–363. https://doi.org/10.1038/43854

Taherkhani, M., Vitousek, S., Barnard, P. L., Frazer, N., Anderson, T. R., & Fletcher, C. H. (2020). Sea-level rise exponentially increases coastal flood frequency. *Scientific Reports*, *10*(1), 1–17. https://doi.org/10.1038/s41598-020-62188-4

Talke, S. A., & Jay, D. A. (2020). Changing Tides: The Role of Natural and Anthropogenic Factors. *Annual Review of Marine Science*, *12*, 121–151. https://doi.org/10.1146/annurev-marine-010419-010727

UNCTAD (2021). *Review of Maritime Transport 2021*. UNCTAD: New York. Retrieved from https://unctad.org/publication/review-maritime-transport-2021

Wahl, T., Haigh, I. D., Nicholls, R. J., Arns, A., Dangendorf, S., Hinkel, J., & Slangen, A. B. A. (2017). Understanding extreme sea levels for broad-scale coastal impact and adaptation analysis. *Nature Communications*, *8*(May), 1–12. https://doi.org/10.1038/ncomms16075

Wang, B., & Fan, Z. (1999). Choice of South Asian Summer Monsoon Indices. Bulletin of the American Meteorological Society, 80(4), 629–638. https://doi.org/10.1175/1520-0477(1999)080<0629:COSASM>2.0.CO;2

Woodworth, P. L., Melet, A., Marcos, M., Ray, R. D., Wöppelmann, G., Sasaki, Y. N., … Merrifield, M. A. (2019). Forcing Factors Affecting Sea Level Changes at the Coast. *Surveys in Geophysics* (Vol. 40). https://doi.org/10.1007/s10712-019-09531-1

Woodworth, P. L. (2022). Advances in the observation and understanding of changes in sea level and tides. *Annals of the New York Academy of Sciences*, *1516*(1), 48–75. https://doi.org/10.1111/nyas.14851

Zhang, H., & Sheng, J. (2015), Examination of extreme sea levels due to storm surges and tides over the northwest Pacific Ocean, *Continental Shelf Research*, *93*(0), 81-97, doi: http://dx.doi.org/10.1016/j.csr.2014.12.001.

Received: 26th June 2023. Accepted: 15th August 2023